HHS Public Access

Author manuscript

Arthritis Rheumatol. Author manuscript; available in PMC 2017 February 01.

Published in final edited form as:

Arthritis Rheumatol. 2016 February ; 68(2): 359–369. doi:10.1002/art.39442.

"Receptor protein tyrosine phosphatase alpha enhances rheumatoid synovial fibroblast signaling and promotes arthritis in mice"

Stephanie M. Stanford, Ph.D.[1], **Mattias N. D. Svensson, Ph.D.**[1], **Cristiano Sacchetti, Ph.D.**[1], **Caila A. Pilo, B.S.**[1], **Dennis J. Wu, B.S.**[1], **William B. Kiosses, Ph.D.**[2], **Annelie Hellvard, Ph.D.**[3], **Brith Bergum, M.Sc.**[3], **German R. Aleman Muench, Ph.D.**[1], **Christian Elly, B.S.**[1], **Yun-Cai Liu, Ph.D.**[1], **Jeroen den Hertog, Ph.D.**[4,5], **Ari Elson, Ph.D.**[6], **Jan Sap, Ph.D.**[7], **Piotr Mydel, M.D., Ph.D.**[3], **David L. Boyle, B.S.**[8], **Maripat Corr, M.D.**[8], **Gary S. Firestein, M.D.**[8], and **Nunzio Bottini, M.D., Ph.D.**[1]

[1]Division of Cellular Biology, La Jolla Institute for Allergy and Immunology, La Jolla, CA [2]Core Microscopy, Scripps Research Institute, La Jolla, CA [3]Broegelmann Research Laboratory, Department of Clinical Science, University of Bergen, Norway [4]Hubrecht Institute-Koninklijke Nederlands Akademie van Wetenschappen and University Medical Center Utrecht, The Netherlands [5]Institute of Biology Leiden, The Netherlands [6]Department of Molecular Genetics, the Weizmann Institute of Science, Rehovot, Israel [7]Université Paris Diderot, Sorbonne Paris Cité, Epigenetics and Cell Fate, Paris, France [8]Division of Rheumatology, Allergy and Immunology, UCSD School of Medicine, La Jolla, CA

Abstract

Objective—During rheumatoid arthritis (RA), fibroblast-like synoviocytes (FLS) critically promote disease pathogenesis by aggressively invading the joint extracellular matrix. The focal adhesion kinase (FAK) signaling pathway is emerging as a contributor to RA FLS anomalous behavior. The receptor protein tyrosine phosphatase α (RPTPα), encoded by the *PTPRA* gene, is a key promoter of FAK signaling. Here we investigated whether RPTPα mediates FLS aggressiveness and RA pathogenesis.

Methods—Through RPTPα knockdown, we assessed FLS gene expression by quantitative polymerase chain reaction and enzyme-linked immunosorbent assay, invasion and migration in transwell assays, survival by Annexin V and propidium iodide staining, adhesion and spreading by immunofluorescence microscopy, and activation of signaling pathways by Western blotting of FLS lysates. Arthritis development was examined in *Ptpra*$^{-/-}$ mice using the K/BxN serum transfer model. The contribution of radiosensitive and radioresistant cells to disease was evaluated by reciprocal bone-marrow transplantation.

Results—RPTPα was enriched in the RA synovial lining. RPTPα knockdown impaired RA FLS survival, spreading, migration, invasiveness and responsiveness to platelet-derived growth factor,

Address correspondence to Nunzio Bottini, M.D., Ph.D., Division of Cellular Biology, La Jolla Institute for Allergy and Immunology, 9420 Athena Circle, La Jolla, CA 92037; Phone: (858) 752-6815, Fax: (858) 752-6895, nunzio@lji.org.

tumor necrosis factor and interleukin-1 stimulation. These phenotypes correlated with increased phosphorylation of SRC on inhibitory Y527 and decreased phosphorylation of FAK on stimulatory Y397. Treatment of RA FLS with an inhibitor of FAK phenocopied knockdown of RPTPα. *Ptpra*-deficient mice were protected from arthritis development, which was due to radioresistant cells.

Conclusions—By regulating phosphorylation of SRC and FAK, RPTPα mediates pro-inflammatory and pro-invasive signaling in RA FLS, correlating with promotion of disease in an FLS-dependent model of RA.

Fibroblast-like synoviocytes (FLS) control the composition of the synovial fluid and extracellular matrix (ECM) of the joint lining. In rheumatoid arthritis (RA), FLS become aggressive and invasive, contributing to disease pathology. FLS produce matrix metalloproteinases (MMPs) that break down the ECM, directly invade and digest the articular cartilage, promote bone erosion, and promote inflammation through secretion of interleukin-6 (IL-6), chemokines, and other inflammatory mediators(1–4). FLS are highly sensitive to the inflammatory environment present in rheumatoid joints. Growth factors, especially platelet-derived growth factor (PDGF), stimulate FLS invasiveness. Inflammatory cytokines, particularly tumor necrosis factor-alpha (TNF) and interleukin-1-beta (IL-1β), enhance FLS aggressiveness, pro-inflammatory features, and MMP production(4). Targeting of molecules that control FLS invasiveness and inflammatory output is considered an option for development of new therapies for RA(4–6).

Many signaling pathways controlling FLS behavior rely upon tyrosine phosphorylation of proteins(4), which results from the balanced action of protein tyrosine kinases (PTKs) and phosphatases (PTPs). The focal adhesion kinase (FAK) pathway is emerging as an important mediator of the anomalous behavior of RA FLS. FAK is a ubiquitously expressed non-receptor tyrosine kinase that acts as a critical mediator of cell motility and invasiveness(7) and promotes cell survival(8). FAK activation is dependent upon tyrosine 397 (Y397) phosphorylation induced by integrin-mediated cell adhesion(7,8). This site can be autophosphorylated by FAK or phosphorylated by SRC family kinases (SFKs), which use phospho-Y397 as a docking site to activate FAK through phosphorylation of other tyrosine residues. Increased phospho-FAK levels were shown in RA synovial lining cells compared to normal tissue(9), and a recent epigenomics study showed that the FAK pathway is a hotspot of epigenetic anomalies in RA FLS(10). These findings suggest that anomalous FAK activation may play a significant role in RA FLS aggressiveness.

We recently reported that the PTP SHP-2, which is overexpressed in RA FLS versus osteoarthritis (OA) FLS, mediates the aggressive RA FLS phenotype by promoting FAK activation, leading to enhanced FLS survival, invasiveness, and responsiveness to PDGF and TNF stimulation(11). We noted that receptor PTP-α (RPTPα), another PTP that regulates FAK activity in fibroblast and solid cancer cell lines(12–14), was also highly expressed in RA FLS(11).

RPTPα, encoded by the *PTPRA* gene, is ubiquitously expressed(15,16). RPTPα is a critical positive regulator of signaling through dephosphorylation of the SFK C-terminal inhibitory tyrosine residue (Y527 in SRC)(13,14,16–18). Dephosphorylation of SRC-Y527 enhances

SRC activation, leading to tyrosine phosphorylation of FAK-Y397 and other substrates. Embryonic fibroblasts from *Ptpra* knockout (KO) mice showed increased SRC-Y527 phosphorylation, reduced SFK activity, reduced FAK-Y397 phosphorylation, and reduced SRC/FAK association(12,14,19). *Ptpra* KO mice were recently reported to be protected from experimentally-induced lung fibrosis, a phenotype mediated by reduced pro-fibrotic transforming growth factor beta (TGFβ) signaling in *Ptpra* KO lung fibroblasts(20). These findings, together with the role for RPTPα in SRC and FAK regulation, and the hypothesized role of the FAK pathway in the pathogenic behavior of RA FLS, led us to investigate a potential role for RPTPα in RA FLS pathophysiology. Here, we demonstrate that RPTPα regulates phosphorylation of SRC and FAK in RA FLS, and promotes RA FLS aggressiveness by mediating signaling in response to TNF, IL-1 and PDGF. We also report that *Ptpra*$^{-/-}$ mice are protected from arthritis in an FLS-dependent model of disease, supporting a model whereby promotion of the FAK pathway by RPTPα in FLS contributes to RA pathogenesis.

Materials and Methods

Antibodies and Other Reagents

The rabbit anti-RPTPα antibody was previously described(14). Other primary antibodies were purchased from Cell Signaling Technology (Danvers, MA) and secondary antibodies from GE Healthcare Life Sciences (Pittsburgh, PA). TNFα, IL-1β and PDGF-BB were purchased from eBioscience (San Diego, CA). The FAK inhibitor PF573228 was purchased from EMD Millipore (Billerca, MA). The AKT inhibitor MK2206 was purchased from SelleckChem (Houston, TX). Unless specified, other reagents were purchased from Sigma-Aldrich (St. Louis, MO).

Immunohistochemistry (IHC) of Synovial Tissue

The anti-RPTPα antibody was optimized for IHC using arthritic ankle sections of WT and *Ptpra* KO mice (data not shown). Paraffin embedded slides of human RA synovial tissues were obtained from the UCSD Clinical and Translational Research Institute (CTRI) Biorepository. Slides were deparaffinated, rehydrated and pretreated for 10 min with boiling citrate antigen retrieval buffer (1.9 mM citric acid, 10 mM Tris-sodium citrate pH 6.0), and treated with 3% H_2O_2 for 10 min. Slides were blocked with 5% goat serum for 1 hr at room temperature, then incubated with rabbit anti-RPTPα antibody or control rabbit IgG (1:100 in 5% bovine serum albumin [BSA]) overnight at 4°C. Slides were washed and incubated with SignalStain Boost IHC Detection reagent (HRP, rabbit) (Cell Signaling Technologies) for 30 min, incubated for 5 min with 3,3’-diaminobenzidine substrate (Sigma-Aldrich), and counterstained with hematoxylin. Slide images were obtained using an Eclipse 80i microscope (Nikon, Melville, NY).

Preparation of FLS

FLS were obtained from the UCSD CTRI Biorepository. Each line was previously obtained from discarded synovial tissue of a different patient with RA at the time of synovectomy, as previously described(21). The diagnosis of RA conformed to American College of Rheumatology 1987 revised criteria(22). FLS were cultured in DMEM (Mediatech,

Manassas, VA) with 10% fetal bovine serum (FBS, Omega Scientific, Tarzana, CA), 2 mM L-glutamine, 50 μg/mL gentamicin, 100 units/ml of penicillin and 100 μg/ml streptomycin (Life Technologies, Carlsbad, CA) at 37°C in a humidified 5% CO_2 atmosphere. For all experiments, FLS were used between passages 4–10, and cells were synchronized in 0.1% FBS (serum-starvation media) for 48 hr prior to analysis or functional assays.

Quantitative Polymerase Chain Reaction (qPCR)

RNA was extracted using RNeasy Kits (Qiagen, Valencia, CA) or Trizol (Life Technologies). For lysis of FLS, adherent cells were first washed in PBS and then lysed in the culture plate. cDNA was synthesized using the SuperScript® III First-Strand Synthesis SuperMix (Life Technologies). qPCR was performed using a Roche Lightcycler 480 (Indianapolis, IN), with primer assays from SABiosciences/Qiagen. Reactions were measured in triplicate and data was normalized to the expression levels of the house-keeping gene glyceraldehyde 3-phosphate dehydrogenase (*GAPDH*) or RNA Polymerase II (*RPII*) (23).

FLS Treatment with Cell-Permeable Antisense Oligonucleotide (PMO)

FLS were treated with 2.5 μM PMO (Gene Tools, Philomath, OR) for 7 days. PMO was replaced in fresh culture medium after 3 days and in serum-starvation medium after 5 days.

Enzyme-Linked Immunosorbent Assay (ELISA)

Secreted human IL-6 and chemokine (C-X-C motif) ligand 10 (CXCL10) were measured using ELISAs from Biolegend (San Diego, CA).

Transwell Invasion Assay

In vitro invasion assays were performed in transwell systems as previously described(24,25). Following treatment with PMO, equal numbers of live RA FLS were resuspended in assay media (DMEM with 0.5% BSA) and allowed to invade through BD BioCoat™ GFR Matrigel™ chambers in response to 50 ng/ml PDGF-BB for 48 hr. Cells were pre-stained with 2 μM CellTracker Green™ or stained post-invasion with 2 μM Hoechst (Life Technologies) for 30 min at room temperature. Fluorescence of invading cells on each membrane was visualized using an Eclipse 80i microscope. Images were acquired from 4 non-overlapping fields per membrane, and invading cells in each field were counted using ImageJ software. Each experiment included 3–4 membranes per sample.

Transwell Migration Assay

Transwell migration assays were similarly performed. Following treatment with PMO, equal numbers of live RA FLS were allowed to migrate through uncoated transwell chambers in response to 5% FBS for 24 hr. Each experiment included 3–4 membranes per sample.

Survival and Apoptosis Assay

Following treatment with PMO, RA FLS were washed and incubated for an additional 24 hr in serum-starvation media. Adherent and non-adherent cells were collected and stained with Annexin V-Alexa Fluor® 647 and propidium iodide (PI) according to the manufacturer's

instructions (Biolegend, San Diego, CA). Cell fluorescence was assessed by FACS using a BD LSR-II (BD Biosciences), and counts and percentages of live (Annexin $V^{-}PI^{-}$), early apoptotic (Annexin $V^{+}PI^{-}$), or late apoptotic/necrotic (Annexin $V^{+}PI^{+}$) cells were obtained. Data was analyzed for statistical significance using the Chi-square test for independence.

Spreading and Adhesion Assay

Following treatment with PMO, equal numbers of live RA FLS were resuspended in FLS medium containing 5% FBS and allowed to adhere onto coverslips coated with 20 μg/ml fibronectin (FN) at 37°C for 15, 30 and 60 min. Cells were fixed in 4% para-formaldehyde for 5 min, permeabilized in 0.2% Triton X-100 for 2 min, and stained with 5 U/ml Alexa Fluor® 568 (AF 568)-conjugated phalloidin and 2 μg/ml Hoechst for 20 min (Life Technologies). Samples were imaged with an Olympus FV10i Laser Scanning Confocal Microscope (Olympus, Center Valley, PA). Using the FV10i acquisition software, each coverslip was separated into four nine-paneled mega-images. Each panel (1024×1024) was acquired with a 10× objective and then stitched together, through a 10% overlap, with the Olympus FluoView 1000 imaging software. Total cell number and cell areas for each panel were calculated using Image Pro Analyzer software (Media Cybernetics, Rockville, MD).

Cell Lysis for Western Blotting (WB)

Adherent cells were washed in PBS and then lysed in the culture plate in RIPA buffer (25 mM Tris-HCl pH 7.6, 150 mM NaCl, 1% NP-40, 1% sodium deoxycholate, 0.1% SDS) containing 1 mM phenylmethanesulfonyl fluoride, 10 μg/ml aprotinin, 10 μg/ml leupeptin, 10 μg/ml soybean trypsin inhibitor, 10 mM sodium orthovanadate, 5 mM sodium fluoride and 2 mM sodium pyrophosphate. Protein concentration of cell lysates was determined using the Pierce BCA Protein Assay Kit (Thermo Scientific, Rockford, IL).

Mice

Animal experiments were conducted in accordance with a La Jolla Institute for Allergy & Immunology (LJI) Institutional Animal Care and Use Committee-approved protocol (#AP140-NB4). *Ptpra* KO mice were generated as previously described(26). C57BL/6 KRN mice were provided by Dr. Christophe Benoist (Harvard Medical School) and were crossed with NOD mice (Jackson Laboratories, Bar Harbor, MN) to obtain arthritic offspring (K/BxN mice) whose sera was pooled for use in the K/BxN passive serum transfer arthritis model(27). Congenic CD45.1 C57BL/6 mice were purchased from Taconic Biosciences (Hudson, NY).

K/BxN Passive Serum Transfer Arthritis Model

Arthritis was induced in 8 week-old mice by intraperitoneal (i.p.) injection of 200 μL pooled sera from K/BxN mice. Every 2 days, ankle thickness was measured using a digital caliper(27).

Reciprocal Bone-Marrow Transplantation

Male recipient mice were lethally irradiated with 2 doses of 550 rads and administered bone-marrow from male donor mice. WT congenic CD45.1 mice were administered bone-marrow

cells from WT or *Ptpra* KO CD45.2 mice, and WT or *Ptpra* KO mice were administered bone-marrow cells from WT congenic CD45.1 mice. KBxN pooled sera was administered to induce arthritis 10–11 weeks post-irradiation. Percentage of engrafted cells in WT recipients reconstituted with KO bone-marrow and in KO recipients reconstituted with WT bone-marrow was >90%.

Assessment of Inflammation with an Intravital Probe

The Xenolight Rediject Inflammation Probe (PerkinElmer, Waltham, MA) is an intravital luminescent dye that penetrates phagocytic cells and enables visualization of joint infiltration. Probe was administered to mice 7 days after arthritis induction by i.p. injection according to the manufacturer's instructions. Joint inflammation was quantified using the Xenogen IVIS Spectrum *in vivo* Imaging System (Perkin Elmer).

Histological Analysis of Arthritic Joints

Hind paws were fixed in 10% neutral-buffered formalin, decalcified and embedded in paraffin. Sections were prepared from the tissue blocks and stained with H&E and Safranin-O/Fast Green/Hematoxylin (HistoTox, Boulder CO). Histopathological scoring was performed as previously described(28). Joints were given scores of 0–4 for bone erosion: 0=normal; 1=minimal (small areas of erosion, not readily apparent on low magnification); 2=mild (more numerous areas of erosion, not readily apparent on low magnification, in trabecular or cortical bone); 3=moderate (obvious erosion of trabecular and cortical bone, without full-thickness cortex defects; loss of some trabeculae; lesions apparent on low magnification); and 4=marked (full-thickness defects in the cortical bone and marked trabecular bone loss). Cartilage depletion was identified by diminished Safranin-O staining of the matrix and was scored on a scale of 0–4: 0=no cartilage destruction (full Safranin-O staining); 1=localized cartilage erosions; 2=more extended cartilage erosions; 3=severe cartilage erosions; and 4=depletion of entire cartilage. Histologic analyses were performed in a blinded manner by 2 independent operators.

Joint Extravasation Assay

Mice were injected retro-orbitally with AngioSense-680 Probe according to the manufacturer's instructions (PerkinElmer), and after 5 min were injected i.p. with arthritogenic K/BxN sera. After 1 hr, joint fluorescence was quantified using the Xenogen IVIS Spectrum.

Statistical Analysis

The two-way analysis of variance, Mann-Whitney test, Wilcoxon matched-pairs signed rank test, and Chi-square test for independence were performed using GraphPad Prism software. A comparison was considered significant if p was less than 0.05.

Results

RPTPα is expressed in fibroblasts from the RA synovium

We first explored a possible role for RPTPα in RA FLS. We previously reported high expression of PTPRA in cultured RA FLS(11). Here, IHC of human RA synovial sections revealed prominent RPTPα expression in the synovial intimal lining (Fig. 1A). We examined if *PTPRA* expression in RA FLS is affected by cell stimulation with inflammatory cytokines, and found that stimulation of RA FLS with TNF and IL-1β had no effect on *PTPRA* expression (data not shown).

RPTPα promotes responsiveness of FLS to inflammatory cytokine stimulation

We next tested the effect of RPTPα deficiency on the response of RA FLS to TNF and IL-1β stimulation. We subjected RA FLS to RPTPα knockdown with cell-permeable antisense oligonucleotide (PMO, Fig. 1B–C). Treatment with PTPRA PMO significantly reduced RA FLS production of *CXCL10* and *MMP13* in response to TNF, and significantly reduced RA FLS production of *IL6*, *CXCL10*, *MMP3* and *MMP13* in response to IL-1β (Fig. 1D). We assessed whether these effects were due to down-regulation of TNF receptor (*TNFRSF1A*) or IL-1β receptor (*IL1R*) expression. We found no effect on expression of *TNFRSF1A*, however PTPRA PMO increased expression of *IL1R* (Fig. 1D). The effect on CXCL10 and IL-6 was further confirmed by treatment of RA FLS with a second PTPRA-targeted PMO of a different sequence (data not shown). Taken together, these data suggest that RPTPα promotes production of pro-inflammatory and pro-invasive mediators by RA FLS in response to inflammatory cytokines. While a role for RPTPα in the regulation of IL-1β signaling has been previously reported(29–31), this is to the best of our knowledge the first report of a role for RPTPα in TNF signaling.

RPTPα promotes RA FLS invasiveness

We next examined if RPTPα affects invasiveness of RA FLS. RA FLS invasiveness *ex vivo* was shown to correlate with radiographic damage during RA progression(25). We subjected PMO-treated RA FLS to transwell invasion assays through Matrigel in response to PDGF, a highly expressed promoter of FLS invasiveness in the RA synovium(4). RA FLS treated with PTPRA PMO, compared to control non-targeting PMO-treated cells, were significantly less invasive in response to PDGF (Fig. 2A; median and IQR % max cells per field 54.4 and 40.3–77.5 for Ctl PMO; 23.8 and 13.7–40.0 for PTPRA PMO, $p<0.05$). We next assessed if the effect of PTPRA PMO on RA FLS invasiveness was due to impaired cell motility. PTPRA PMO-treated cells showed significantly reduced migration in a transwell assay in response to 5% FBS (Fig. 2B; median and IQR % max cells per field 49.4 and 29.8–64.9 for Ctl PMO; 16.1 and 11.4–24.5 for PTPRA PMO). We hypothesized this could be due to increased cell death or to reduced cytoskeletal reorganization following RPTPα knockdown. We therefore assayed the effect of PTPRA PMO on cell apoptosis and necrosis, and on cell spreading. RA FLS treated with PTPRA PMO showed significantly increased apoptosis compared to control-treated cells in sera-starvation media (data not shown) or in the presence of PDGF (Fig. 2C). We also found that live PTPRA PMO-treated cells were less adherent to, and displayed impaired spreading on, fibronectin-coated coverslips (Fig. 2D).

Taken together, these data strongly support a role for RPTPα in promoting RA FLS survival and growth factor-dependent cytoskeletal reorganization, migration and invasiveness.

RPTPα promotes RA FLS aggressiveness through control of SRC and FAK activation

The inhibitory SRC tyrosine residue (Y527) was identified as the physiological substrate of RPTPα in multiple cell types(14,16). Dephosphorylation of SRC-Y527 enhances SRC activation, leading to tyrosine phosphorylation of FAK-Y397 –a substrate of SRC(7)- and other SRC substrates. In RA FLS, phospho-SRC-Y527 is constitutive and not induced by TNF or IL-1β stimulation (data not shown). Hypothesizing that RPTPα dephosphorylates phospho-SRC-Y527 in RA FLS, we assessed whether RPTPα knockdown in RA FLS influences basal SRC-Y527 phosphorylation levels, and found that RPTPα knockdown increased phosphorylation of SRC-Y527 in resting RA FLS (Fig. 3A). We next assessed whether RPTPα knockdown affected signaling downstream SRC in RA FLS. We found that FAK-Y397 was constitutively phosphorylated in RA FLS. Phospho-FAK-Y397 was unaffected by TNF and IL-1β stimulation and its phosphorylation was reduced by RPTPα knockdown (Fig. 3C). As FAK promotes activation of mitogen-activated protein kinases (MAPKs)(7), and is critical for JNK activation in RA FLS(32), we next examined if RPTPα knockdown affected TNF- and IL-1β-induced activation of the JNK and p38 MAPKs. We found RPTPα knockdown impaired TNF- and IL-1β-stimulated phosphorylation of the activation motif of JNK (T183/Y185) and also p38-T180/Y182 (Fig. 3B–C and data not shown). We also examined whether RPTPα promoted activation of the AKT and NF-κB signaling pathways, which are activated by inflammatory cytokine stimulation in RA FLS(4). As shown in Fig. 3B–C, PTPRA PMO treatment reduced TNF- and IL-1β stimulated phosphorylation of AKT-S473. Interestingly, PTPRA PMO treatment caused a modest decrease in the levels of IκBα protein in resting RA FLS. Stimulation of cells with TNF or IL-1β, however caused degradation of IκBα protein in both Ctl and PTPRA PMO-treated cells, and by 10 minutes post-stimulation the levels of IκBα were similar between Ctl and PTPRA PMO-treated cells (Fig. 3B–C and data not shown). The trend of decreased basal levels of IκBα in PTPRA PMO-treated cells was not accompanied by increased basal activation of the NFκB pathway, but rather we found a non-significant trend towards decreased basal phosphorylation of IκB kinase (IKK)-αβ on Ser176/180 and NFκB subunit p65 on Ser536 (Fig. 3D). Additionally, we found that proteolytic processing of NFκB subunits p100 and p105 -as assessed by the ratio of p52:p100 or p50:p105, respectively- in basal conditions was unaffected by PTPRA knockdown (data not shown).

We next tested whether FAK or AKT play essential roles in RA FLS induction of gene expression in response to TNF and IL-1 using pharmacological inhibitors. Similar to the effect of RPTPα knockdown (Fig. 1D), treatment of RA FLS with the FAK inhibitor PF573228 led to significantly decreased TNF- and IL-1-induced production of *CXCL10*, *IL6* and *MMP13* (Fig. 4A). On the contrary, treatment with the AKT inhibitor MK2206 did not dampen expression of any these genes, but rather increased expression of *IL6* and IL-1β-induced expression of *CXCL10* (Fig. 4A). We then further examined the effect of the FAK inhibitor PF573228 on RA FLS signaling. We confirmed that treatment of RA FLS with PF573228 does not cause death of RA FLS at the concentrations used in these experiments (data not shown). We found that treatment of RA FLS with PF573228 impaired FAK-Y397

phosphorylation and TNF- and IL-1β-induced phosphorylation of JNK-T183/Y185 (Fig. 4B), but had no effect on p38-T180/Y185 phosphorylation. These findings strongly suggest that RPTPα promotes TNF- and IL-1β-stimulated production of CXCL10, IL-6 and MMP-13 through a SRC-FAK-JNK signaling pathway. RPTPα also likely promotes other signaling pathways in RA FLS -such as the AKT and p38 pathways- that are independent of FAK. Taken together, these data suggest a model whereby RPTPα mediates RA FLS aggressiveness by promoting constitutive activation of SRC and FAK, leading to enhanced FLS survival, increased production of critical mediators of arthritis in response to TNF and IL-1β, and promotion of motility and invasiveness in response to PDGF.

Ptpra KO mice are resistant to K/BxN passive transfer arthritis through an effect on radioresistant cells

Having determined that RPTPα regulates the aggressive behavior of FLS *ex vivo*, we asked whether RPTPα mediates the pathogenic behavior of FLS in RA. We subjected wild-type (WT) and *Ptpra* KO mice to the FLS-dependent K/BxN serum transfer model of inflammatory arthritis and followed disease course for 2 weeks. *Ptpra* KO mice displayed significantly decreased arthritis severity as assessed by measurements of ankle swelling (Fig. 5A), joint inflammation using an intravital probe (Fig. 5B), and bone and cartilage erosions (Fig. 5C). *Ptpra* KO does not cause a bone phenotype *per se*(33), suggesting that RPTPα promotes K/BxN serum-induced bone erosion through an effect on inflammation.

In the K/BxN serum transfer model, disease development depends primarily upon actions of innate immune cells and FLS(34–36). To determine whether disease protection in the *Ptpra* KO mouse is due to recruited myeloid cells or radioresistant cells, such as FLS, we performed reciprocal bone-marrow transplantation. WT recipient mice showed no difference in arthritis severity after transplantation with bone-marrow from WT or *Ptpra* KO donor mice (Fig. 6A). However, *Ptpra* KO mice still showed significantly reduced severity of arthritis compared to WT mice after transplantation with bone-marrow from WT mice (Fig. 6B). These data suggest that arthritis in this model is promoted by *Ptpra* through an effect on radioresistant cells. To rule out effects of RPTPα on radioresistant cell types that control vascular permeability, we examined whether *Ptpra* KO reduced acute K/BxN serum-induced extravasation to the ankles, and found no effect of *Ptpra* KO using an intravital tracer (Fig. 6C). Finally, upon examination of the expression of pathogenic mediators of disease in arthritic ankle homogenates, we found that *Ptpra* KO mice exhibited significantly reduced expression of several genes produced by FLS during arthritis, including *Il6* and *Mmp3* –two important mediators of joint destruction in RA(4,37)- and *Cxcl10* –a critical pathogenic factor in mouse and human RA(38,39) (Fig. 6D). *Ptpra* KO mice also exhibited slightly reduced expression of *Tnf* and *Il1b* –inflammatory cytokines produced by immune cells that drive disease in the K/BxN model (Fig. 6D) -likely a secondary phenomenon due to decreased inflammatory infiltrate in the *Ptpra* KO joint.

Discussion

We report the first characterization of the role of RPTPα in FLS and in RA. RPTPα is expressed in the primary rheumatoid synovium and in cultured FLS. Knockdown of RPTPα

expression impaired RA FLS induction of pro-inflammatory and pro-invasive factors in response to TNF or IL-1β stimulation. Additionally, RPTPα knockdown reduced RA FLS invasiveness in response to PDGF, which is attributed to a combination of decreased survival, cytoskeletal reorganization and motility. We assessed whether RPTPα mediates arthritis severity in the K/BxN mouse model, where FLS are critical to disease development(35). *Ptpra* deletion significantly reduced arthritis development, which reciprocal bone-marrow transplantation revealed was due to radioresistant cells.

The observed decreased invasiveness, motility and survival of RA FLS subjected to RPTPα knockdown is consistent with previous reports on the regulation of the SRC/FAK pathway by RPTPα in other fibroblasts(14,16). In line with these reports, we observed that in resting RA FLS, loss of RPTPα increased phosphorylation of SRC-Y527 and impaired FAK-Y397 phosphorylation. We next investigated the RPTPα-regulated pathways downstream TNF and IL-1β, and found that RPTPα knockdown reduced JNK, p38 and AKT phosphorylation after TNF and IL-1β stimulation. Through the use of chemical inhibitors we identified the FAK-JNK pathway as responsible for the effect of RPTPα on expression of *CXCL10*, *IL6* and *MMP13* after TNF and IL-1β stimulation. The observed increase in *IL6* expression after RA FLS treatment with the AKT inhibitor is interesting given that this compound has been shown to attenuate RA FLS migration and invasiveness(40). The effect on IL-6 suggests that the AKT pathway can have differential effects on FLS aggressive phenotypes. The effect of RPTPα on AKT and p38 signaling warrants further future investigation.

Our experiments strongly suggest that FLS at least in part mediate the reduced arthritis severity in *Ptpra* KO mice. We can reasonably rule out that RPTPα promotes inflammation mediated by neutrophils, macrophages, or platelets, three radiosensitive cell types that contribute to pathogenicity in the K/BxN model(41–43). An effect on endothelial cells also is unlikely since in our experiments RPTPα did not affect K/BxN serum-induced vascular permeability. Mast cells are relatively radioresistant and have a controversial role in the K/BxN model(44); however *Ptpra* KO mice displayed increased IgE-dependent anaphylaxis, suggesting *Ptpra* deletion does not suppress mast cell function(45). Since disease pathogenesis in the passive K/BxN model is lymphocyte-independent(36), this model has not allowed us to examine whether there is a role for RPTPα in lymphocyte-mediated RA pathogenesis. However, peripheral T cell activation and proliferation were shown to be unaffected by *Ptpra* deletion(46). Since phospho-SRC-Y527 is also targeted by the highly expressed PTP CD45, which is only present in hematopoietic cells, it is likely that redundancy between RPTPα and CD45 renders RPTPα less critical in adaptive immune cell signaling. Indeed, CD45 was reported to display much higher activity than RPTPα in T cells(47).

It was recently reported that *Fak* deletion reduced FLS migration and invasiveness, however global *Fak* KO did not affect disease severity in a TNF-induced mouse arthritis model(48). A possible explanation for the difference in arthritis phenotypes between *Ptpra* and *Fak* KO mice could be that deletion of *Fak* has opposing effects in FLS versus other arthritis-relevant cell types–such as immune cells. Thus, we speculate that *Ptpra KO* mice do not phenocopy *Fak* KO mice because *Ptpra* deletion affects FAK signaling in non-immunological cell types only.

This study suggests inhibiting RPTPα may be therapeutically beneficial for RA. The recent report that *Ptpra* KO mice are protected from fibrosis in a systemic sclerosis model(20) indicates that RPTPα could be an attractive target for combating other autoimmune diseases. Since these studies involved global *Ptpra* deletion from the embryonic stage, determining if acute deletion or pharmacological inhibition of *Ptpra* in adult mice reverses established disease will be helpful in assessing whether RPTPα holds value as a therapeutic target. Additionally, since RPTPα promotes growth of transformed cells, it is also considered a potential drug target for cancer(49,50). Taken together, these findings suggest that exploration of the therapeutic potential of RPTPα is warranted.

Acknowledgments

The authors are grateful to the UCSD CTRI Biorepository for the FLS lines, to Dr. Catherine Pallen for critical review of the data, and to Jay Sharma for data collection. This is manuscript #1111 from LJI.

This work was supported by LJI Institutional funding (N.B.) and NIH (N.B.: AR066053; G.S.F.: AR47825, AI070555, and Clinical and Translational Science Award UL1TR000100).

References

1. Ospelt C, Neidhart M, Gay RE, Gay S. Synovial activation in rheumatoid arthritis. Frontiers in bioscience: a journal and virtual library. 2004; 9:2323–2334. [PubMed: 15353290]
2. Lefevre S, Knedla A, Tennie C, Kampmann A, Wunrau C, Dinser R, et al. Synovial fibroblasts spread rheumatoid arthritis to unaffected joints. Nature medicine. 2009; 15(12):1414–1420.
3. Neumann E, Lefevre S, Zimmermann B, Gay S, Muller-Ladner U. Rheumatoid arthritis progression mediated by activated synovial fibroblasts. Trends Mol Med. 2010; 16(10):458–468. [PubMed: 20739221]
4. Bottini N, Firestein GS. Duality of fibroblast-like synoviocytes in RA: passive responders and imprinted aggressors. Nat Rev Rheumatol. 2013; 9(1):24–33. [PubMed: 23147896]
5. Noss EH, Brenner MB. The role and therapeutic implications of fibroblast-like synoviocytes in inflammation and cartilage erosion in rheumatoid arthritis. Immunological reviews. 2008; 223:252–270. [PubMed: 18613841]
6. Niedermeier M, Pap T, Korb A. Therapeutic opportunities in fibroblasts in inflammatory arthritis. Best Pract Res Clin Rheumatol. 2010; 24(4):527–540. [PubMed: 20732650]
7. Mitra SK, Hanson DA, Schlaepfer DD. Focal adhesion kinase: in command and control of cell motility. Nature reviews. Molecular cell biology. 2005; 6(1):56–68. [PubMed: 15688067]
8. Hanks SK, Ryzhova L, Shin NY, Brabek J. Focal adhesion kinase signaling activities and their implications in the control of cell survival and motility. Frontiers in bioscience : a journal and virtual library. 2003; 8:d982–d996. [PubMed: 12700132]
9. Shahrara S, Castro-Rueda HP, Haines GK, Koch AE. Differential expression of the FAK family kinases in rheumatoid arthritis and osteoarthritis synovial tissues. Arthritis research & therapy. 2007; 9(5):R112. [PubMed: 17963503]
10. Nakano K, Whitaker JW, Boyle DL, Wang W, Firestein GS. DNA methylome signature in rheumatoid arthritis. Ann Rheum Dis. 2013; 72(1):110–117. [PubMed: 22736089]
11. Stanford SM, Maestre MF, Campbell AM, Bartok B, Kiosses WB, Boyle DL, et al. Protein tyrosine phosphatase expression profile of rheumatoid arthritis fibroblast-like synoviocytes: a novel role of SH2 domain-containing phosphatase 2 as a modulator of invasion and survival. Arthritis Rheum. 2013; 65(5):1171–1180. [PubMed: 23335101]
12. Zeng L, Si X, Yu WP, Le HT, Ng KP, Teng RM, et al. PTP alpha regulates integrin-stimulated FAK autophosphorylation and cytoskeletal rearrangement in cell spreading and migration. J Cell Biol. 2003; 160(1):137–146. [PubMed: 12515828]

13. Cheng SY, Sun G, Schlaepfer DD, Pallen CJ. Grb2 promotes integrin-induced focal adhesion kinase (FAK) autophosphorylation and directs the phosphorylation of protein tyrosine phosphatase alpha by the Src-FAK kinase complex. Mol Cell Biol. 2014; 34(3):348–361. [PubMed: 24248601]
14. Su J, Muranjan M, Sap J. Receptor protein tyrosine phosphatase alpha activates Src-family kinases and controls integrin-mediated responses in fibroblasts. Curr Biol. 1999; 9(10):505–511. [PubMed: 10339427]
15. Sap J, D'Eustachio P, Givol D, Schlessinger J. Cloning and expression of a widely expressed receptor tyrosine phosphatase. Proc Natl Acad Sci U S A. 1990; 87(16):6112–6116. [PubMed: 2166945]
16. Pallen CJ. Protein tyrosine phosphatase alpha (PTPalpha): a Src family kinase activator and mediator of multiple biological effects. Curr Top Med Chem. 2003; 3(7):821–835. [PubMed: 12678847]
17. Zheng XM, Wang Y, Pallen CJ. Cell transformation and activation of pp60c-src by overexpression of a protein tyrosine phosphatase. Nature. 1992; 359(6393):336–339. [PubMed: 1383828]
18. den Hertog J, Pals CE, Peppelenbosch MP, Tertoolen LG, de Laat SW, Kruijer W. Receptor protein tyrosine phosphatase alpha activates pp60c-src and is involved in neuronal differentiation. EMBO J. 1993; 12(10):3789–3798. [PubMed: 7691597]
19. Ponniah S, Wang DZ, Lim KL, Pallen CJ. Targeted disruption of the tyrosine phosphatase PTPalpha leads to constitutive downregulation of the kinases Src and Fyn. Curr Biol. 1999; 9(10): 535–538. [PubMed: 10339428]
20. Aschner Y, Khalifah AP, Briones N, Yamashita C, Dolgonos L, Young SK, et al. Protein tyrosine phosphatase alpha mediates profibrotic signaling in lung fibroblasts through TGF-beta responsiveness. Am J Pathol. 2014; 184(5):1489–1502. [PubMed: 24650563]
21. Alvaro-Gracia JM, Zvaifler NJ, Brown CB, Kaushansky K, Firestein GS. Cytokines in chronic inflammatory arthritis. VI. Analysis of the synovial cells involved in granulocyte-macrophage colony-stimulating factor production and gene expression in rheumatoid arthritis and its regulation by IL-1 and tumor necrosis factor-alpha. Journal of immunology. 1991; 146(10):3365–3371.
22. Arnett FC, Edworthy SM, Bloch DA, McShane DJ, Fries JF, Cooper NS, et al. The American Rheumatism Association 1987 revised criteria for the classification of rheumatoid arthritis. Arthritis and rheumatism. 1988; 31(3):315–324. [PubMed: 3358796]
23. Radonic A, Thulke S, Mackay IM, Landt O, Siegert W, Nitsche A. Guideline to reference gene selection for quantitative real-time PCR. Biochemical and biophysical research communications. 2004; 313(4):856–862. [PubMed: 14706621]
24. Laragione T, Brenner M, Mello A, Symons M, Gulko PS. The arthritis severity locus Cia5d is a novel genetic regulator of the invasive properties of synovial fibroblasts. Arthritis and rheumatism. 2008; 58(8):2296–2306. [PubMed: 18668563]
25. Tolboom TC, van der Helm-Van Mil AH, Nelissen RG, Breedveld FC, Toes RE, Huizinga TW. Invasiveness of fibroblast-like synoviocytes is an individual patient characteristic associated with the rate of joint destruction in patients with rheumatoid arthritis. Arthritis and rheumatism. 2005; 52(7):1999–2002. [PubMed: 15986342]
26. Bodrikov V, Leshchyns'ka I, Sytnyk V, Overvoorde J, den Hertog J, Schachner M. RPTPalpha is essential for NCAM-mediated p59fyn activation and neurite elongation. J Cell Biol. 2005; 168(1): 127–139. [PubMed: 15623578]
27. Monach PA, Mathis D, Benoist C. The K/BxN arthritis model. Curr Protoc Immunol. 2008; Chapter 15(Unit 15 22)
28. Guma M, Ronacher L, Liu-Bryan R, Takai S, Karin M, Corr M. Caspase 1-independent activation of interleukin-1beta in neutrophil-predominant inflammation. Arthritis Rheum. 2009; 60(12): 3642–3650. [PubMed: 19950258]
29. Wang Q, Rajshankar D, Branch DR, Siminovitch KA, Herrera Abreu MT, Downey GP, et al. Protein-tyrosine phosphatase-alpha and Src functionally link focal adhesions to the endoplasmic reticulum to mediate interleukin-1-induced Ca2+ signaling. J Biol Chem. 2009; 284(31):20763–20772. [PubMed: 19497848]
30. Wang Q, Rajshankar D, Laschinger C, Talior-Volodarsky I, Wang Y, Downey GP, et al. Importance of protein-tyrosine phosphatase-alpha catalytic domains for interactions with SHP-2

and interleukin-1-induced matrix metalloproteinase-3 expression. J Biol Chem. 2010; 285(29): 22308–22317. [PubMed: 20472558]

31. Rajshankar D, Sima C, Wang Q, Goldberg SR, Kazembe M, Wang Y, et al. Role of PTPalpha in the destruction of periodontal connective tissues. PLoS One. 2013; 8(8):e70659. [PubMed: 23940616]
32. Stanford SM, Aleman Muench GR, Bartok B, Sacchetti C, Kiosses WB, Sharma J, et al. TGFbeta responsive tyrosine phosphatase promotes rheumatoid synovial fibroblast invasiveness. Ann Rheum Dis. 2014
33. Finkelshtein E, Lotinun S, Levy-Apter E, Arman E, den Hertog J, Baron R, et al. Protein tyrosine phosphatases epsilon and alpha perform nonredundant roles in osteoclasts. Mol Biol Cell. 2014; 25(11):1808–1818. [PubMed: 24694598]
34. Ji H, Ohmura K, Mahmood U, Lee DM, Hofhuis FM, Boackle SA, et al. Arthritis critically dependent on innate immune system players. Immunity. 2002; 16(2):157–168. [PubMed: 11869678]
35. Lee DM, Kiener HP, Agarwal SK, Noss EH, Watts GF, Chisaka O, et al. Cadherin-11 in synovial lining formation and pathology in arthritis. Science. 2007; 315(5814):1006–1010. [PubMed: 17255475]
36. Wang Y, Shaked I, Stanford SM, Zhou W, Curtsinger JM, Mikulski Z, et al. The autoimmunity-associated gene PTPN22 potentiates toll-like receptor-driven, type 1 interferon-dependent immunity. Immunity. 2013; 39(1):111–122. [PubMed: 23871208]
37. Baumann H, Kushner I. Production of interleukin-6 by synovial fibroblasts in rheumatoid arthritis. Am J Pathol. 1998; 152(3):641–644. [PubMed: 9502403]
38. Hanaoka R, Kasama T, Muramatsu M, Yajima N, Shiozawa F, Miwa Y, et al. A novel mechanism for the regulation of IFN-gamma inducible protein-10 expression in rheumatoid arthritis. Arthritis Res Ther. 2003; 5(2):R74–R81. [PubMed: 12718750]
39. Lee EY, Lee ZH, Song YW. The interaction between CXCL10 and cytokines in chronic inflammatory arthritis. Autoimmun Rev. 2013; 12(5):554–557. [PubMed: 23092582]
40. Fan W, Zhou ZY, Huang XF, Bao CD, Du F. Deoxycytidine kinase promotes the migration and invasion of fibroblast-like synoviocytes from rheumatoid arthritis patients. Int J Clin Exp Pathol. 2013; 6(12):2733–2744. [PubMed: 24294360]
41. Wipke BT, Allen PM. Essential role of neutrophils in the initiation and progression of a murine model of rheumatoid arthritis. J Immunol. 2001; 167(3):1601–1608. [PubMed: 11466382]
42. Boilard E, Nigrovic PA, Larabee K, Watts GF, Coblyn JS, Weinblatt ME, et al. Platelets amplify inflammation in arthritis via collagen-dependent microparticle production. Science. 2010; 327(5965):580–583. [PubMed: 20110505]
43. Guma M, Hammaker D, Topolewski K, Corr M, Boyle DL, Karin M, et al. Antiinflammatory functions of p38 in mouse models of rheumatoid arthritis: advantages of targeting upstream kinases MKK-3 or MKKk-6. Arthritis and rheumatism. 2012; 64(9):2887–2895. [PubMed: 22488549]
44. Nigrovic PA, Malbec O, Lu B, Markiewski MM, Kepley C, Gerard N, et al. C5a receptor enables participation of mast cells in immune complex arthritis independently of Fcgamma receptor modulation. Arthritis Rheum. 2010; 62(11):3322–3333. [PubMed: 20662064]
45. Samayawardhena LA, Pallen CJ. PTPalpha activates Lyn and Fyn and suppresses Hck to negatively regulate FcepsilonRI-dependent mast cell activation and allergic responses. J Immunol. 2010; 185(10):5993–6002. [PubMed: 20944008]
46. Maksumova L, Le HT, Muratkhodjaev F, Davidson D, Veillette A, Pallen CJ. Protein tyrosine phosphatase alpha regulates Fyn activity and Cbp/PAG phosphorylation in thymocyte lipid rafts. J Immunol. 2005; 175(12):7947–7956. [PubMed: 16339530]
47. Ng DH, Jabali MD, Maiti A, Borodchak P, Harder KW, Brocker T, et al. CD45 and RPTPalpha display different protein tyrosine phosphatase activities in T lymphocytes. Biochem J. 1997; 327(Pt 3):867–876. [PubMed: 9581568]
48. Shelef MA, Bennin DA, Yasmin N, Warner TF, Ludwig T, Beggs HE, et al. Focal adhesion kinase is required for synovial fibroblast invasion, but not murine inflammatory arthritis. Arthritis Res Ther. 2014; 16(5):464. [PubMed: 25280866]

49. Gil-Henn H, Elson A. Tyrosine phosphatase-epsilon activates Src and supports the transformed phenotype of Neu-induced mammary tumor cells. J Biol Chem. 2003; 278(18):15579–15586. [PubMed: 12598528]

50. Zheng X, Resnick RJ, Shalloway D. Apoptosis of estrogen-receptor negative breast cancer and colon cancer cell lines by PTP alpha and src RNAi. Int J Cancer. 2008; 122(9):1999–2007. [PubMed: 18183590]

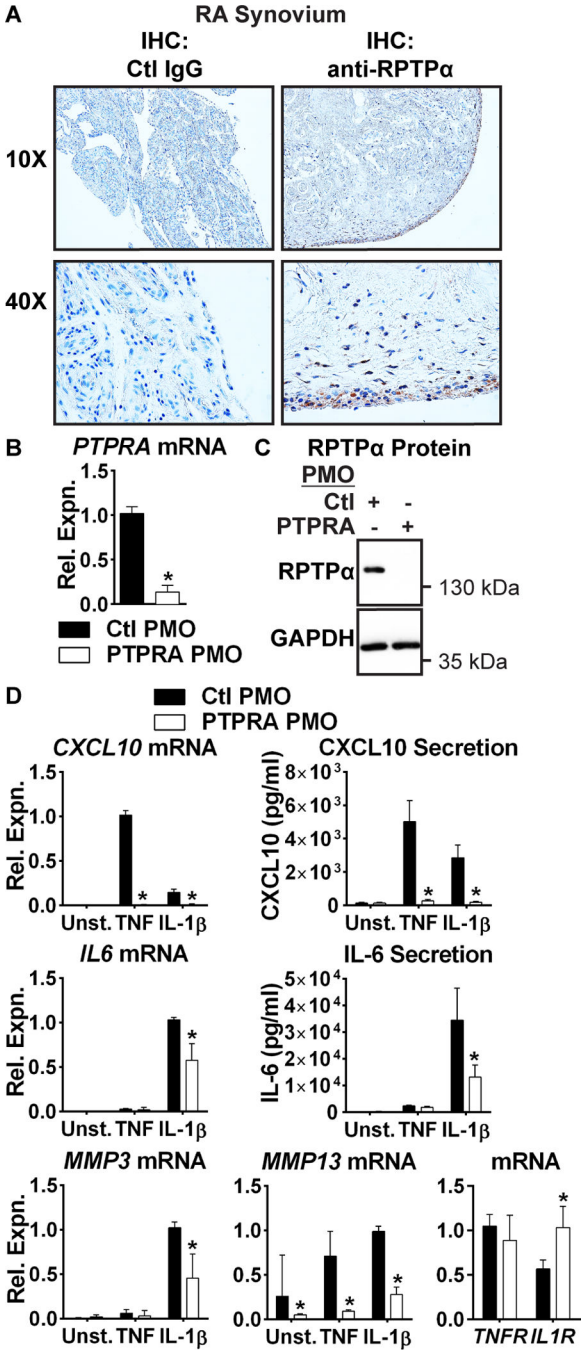

Figure 1. RPTPα is enriched in the RA synovial lining and promotes TNF and IL-1β signaling in RA FLS

(A) Immunohistochemical staining of RA synovial sections using anti-RPTPα or control IgG antibodies. **(B–C)** RA FLS (n=4) were treated with 2.5 μM control non-targeting (Ctl) or PTPRA PMO for 7 d. **(B)** *PTPRA* mRNA expression levels were measured by qPCR. Median and interquartile range (IQR) is shown. *, $p<0.05$, Mann-Whitney test. **(C)** RPTPα protein levels were measured by Western blotting. **(D)** Following treatment with PMO, RA FLS (n=4) were stimulated with 50 ng/ml TNF or 2 ng/ml IL-1 for 24 hr. mRNA expression

was analyzed by qPCR. Median and IQR is shown. Protein expression in cell supernatants was measured by ELISA. Mean ± standard error of the mean (SEM) is shown. *, $p<0.05$, Mann-Whitney test.

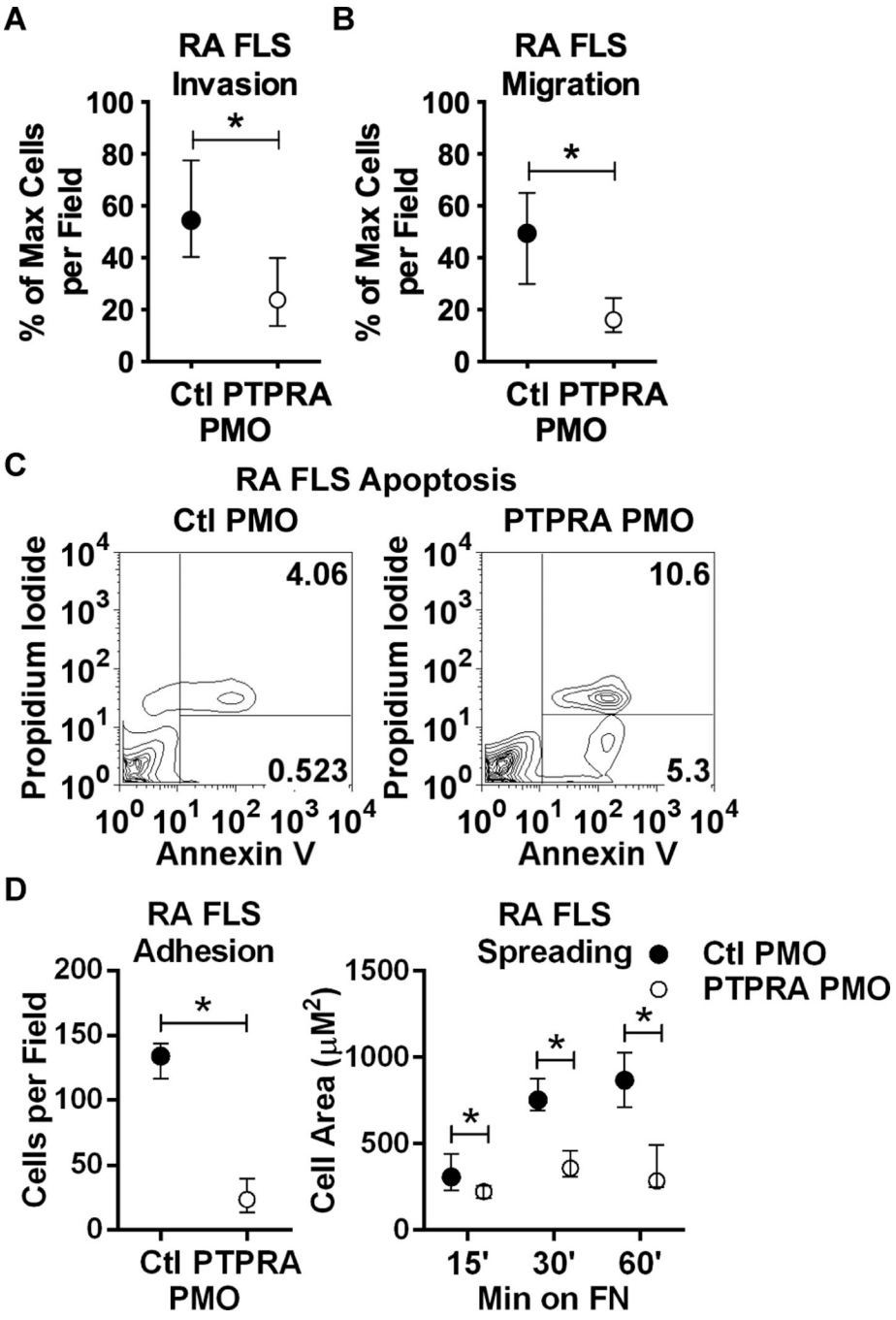

Figure 2. RPTPα promotes RA FLS invasiveness

(A) Following treatment with PMO for 7 d, RA FLS (n=4) invaded through Matrigel-coated transwell chambers in response to 50 ng/ml PDGF-BB for 48 hr. **(B)** PMO-treated RA FLS (n=4) migrated through uncoated transwell chambers in response to 5% FBS for 24 hr. **(A–B)** Median and IQR % maximum number of cells per field is shown. *, $p<0.05$, Mann-Whitney test. **(C)** PMO-treated RA FLS were washed and stimulated with 50 ng/ml PDGF for 24 hr. Cells were collected and stained with Annexin V and PI, and cell fluorescence was assessed by FACS. Graphs show gating strategy to detect early apoptotic (Annexin V^+PI^-)

and necrotic/late apoptotic (Annexin V^+PI^+) cells. Significance was calculated using the Chi square test ($p<0.0001$, Chi-square=2294, df=2). Data is representative of 4 independent experiments. **(D)** PMO-treated RA FLS (n=4) were plated on fibronectin (FN)-coated coverslips in the presence of 5% FBS. Graphs show median and IQR cells per field after 15 min (left) or cell area after 15, 30 and 60 min (right). *, $p<0.05$, Wilcoxon matched-pairs signed rank test.

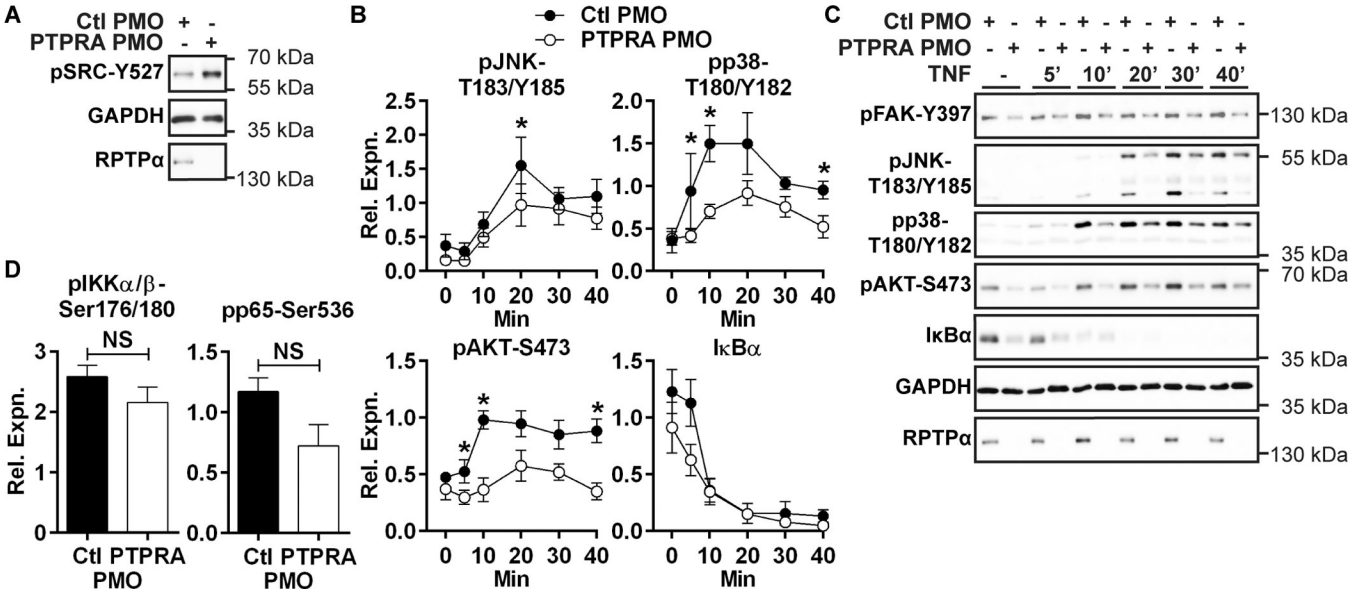

Figure 3. RPTPα promotes RA FLS signaling downstream SRC

(A) anti-pSRC-Y527 levels in PMO-treated RA FLS lysates were measured by Western blotting. Data is representative of 4 independent experiments. **(B–C)** Western blotting of lysates of PMO-treated RA FLS stimulated with 50 ng/ml TNF or left unstimulated. **(B)** Signal intensities of Western blots of TNF-activated proteins from lysates were quantified by densitometric scanning. Mean ± SEM of signal relative to GAPDH from 6 RA FLS lines is shown. **(C)** Representative image is shown. **(D)** Signal intensities of Western blots of lysates from unstimulated PMO-treated RA FLS. Mean ± SEM of signal relative to p65 from 6 RA FLS lines is shown. *, $p<0.05$; NS, non-significant, Wilcoxon matched-pairs signed rank test.

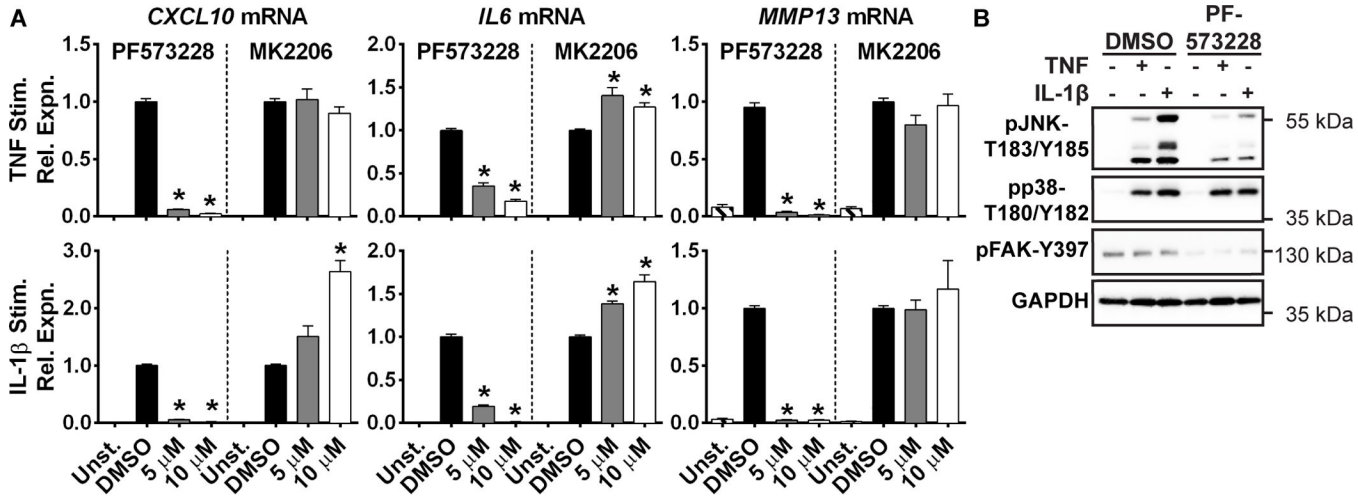

Figure 4. FAK inhibition impairs activation of JNK and TNF and IL-1β-induced gene expression in RA FLS

(A) RA FLS (n=4) were stimulated with 50 ng/ml TNFα or 2 ng/ml IL-1β in the presence of DMSO, the FAK inhibitor PF573228, or the AKT inhibitor MK2206 for 24 hr. mRNA expression was analyzed by qPCR. Mean ± SEM is shown. *, $p<0.05$, Mann-Whitney test. **(B)** RA FLS were stimulated with 50 ng/ml TNF or 2 ng/ml IL-1β for 30 min or left unstimulated, in the presence of DMSO or 10 μM FAK inhibitor PF573228. Data is representative of 4 independent experiments.

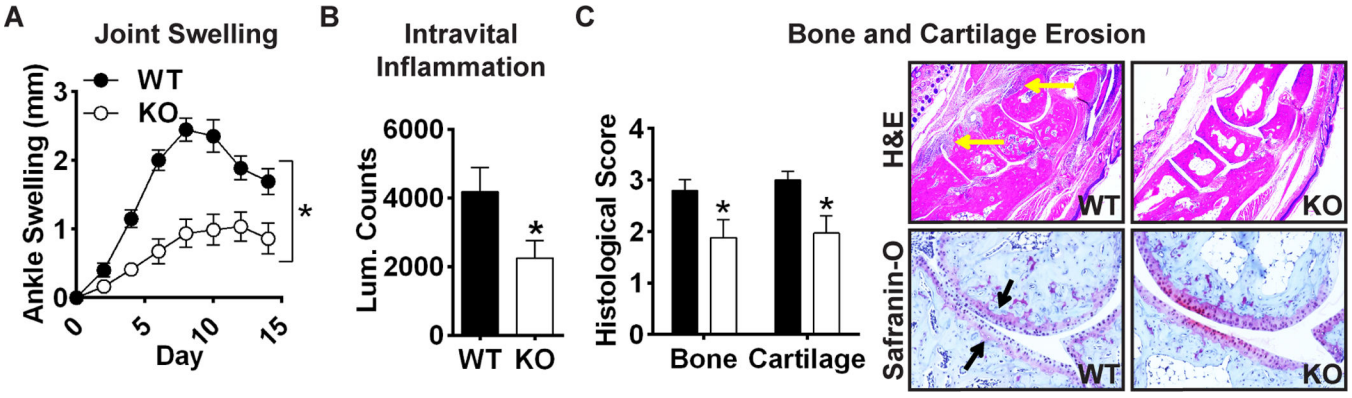

Figure 5. *Ptpra* KO mice are resistant to K/BxN serum transfer arthritis

WT and *Ptpra* KO littermate mice were administered 200 μl K/BxN sera at 8 weeks of age. **(A)** Ankle thickness was measured every 2 days (WT, n=16; KO, n=17). Mean ± SEM ankle swelling is shown. *, $p<0.05$, 2way ANOVA. **(B)** 7 days post-sera transfer, mice (n=3) were injected with intravital inflammation probe and luminescence of wrist and ankle joints was measured. Mean ± SEM luminescent counts per joint are shown. *, $p<0.05$, Wilcoxon matched-pairs signed rank test. **(C)** Histological analysis of ankles stained with H&E or Safranin-O at the end of the disease course. *Left*, histological scores of bone and cartilage erosions (WT, n=16; KO, n=17). Mean ± SEM is shown. *, $p<0.05$, Wilcoxon matched-pairs signed rank test. *Right*, representative images of H&E-stained (upper panels; yellow arrows indicate regions of inflammatory infiltrate) or Safranin-O-stained (lower panels; black arrows indicate regions of cartilage erosion) joints.

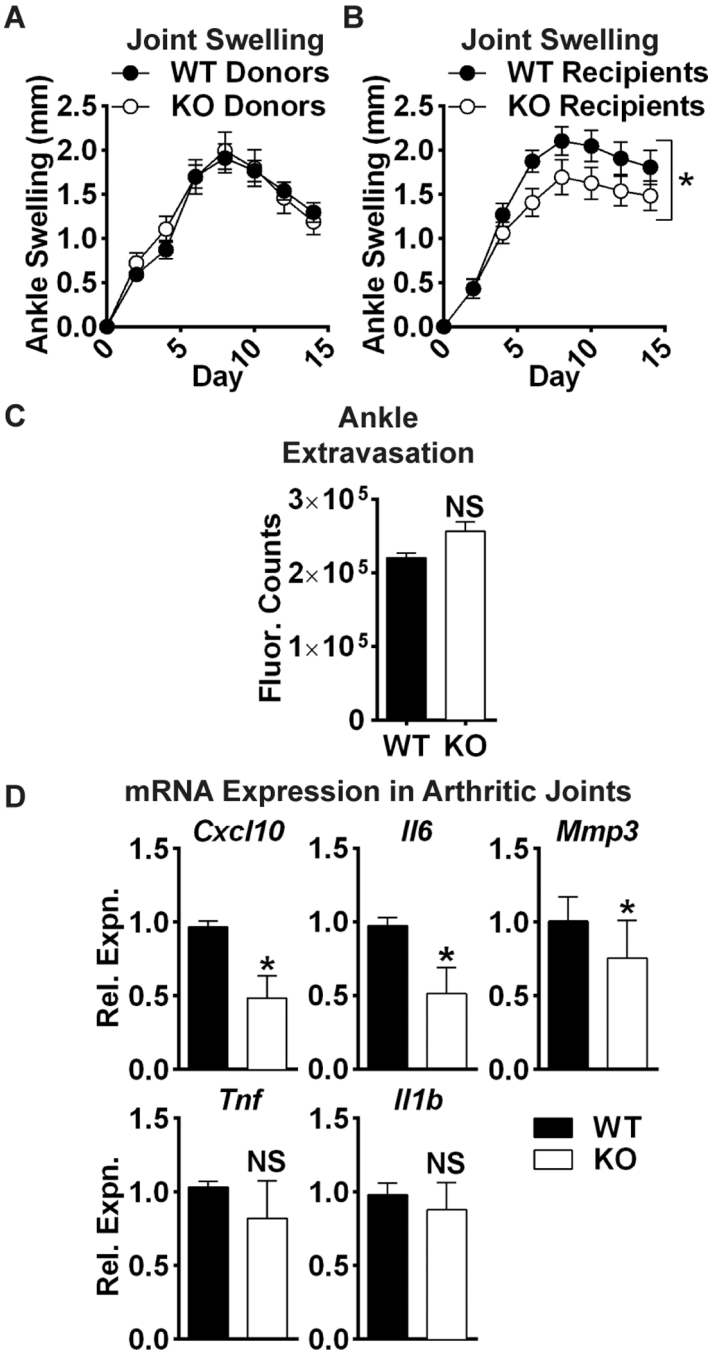

Fig. 6. Arthritis protection in *Ptpra* KO mice is dependent upon radioresistant cells

(A–B) Mice were lethally irradiated and administered bone-marrow from donor mice. 10–11 weeks post-irradiation, arthritis was induced in recipients by administration of K/BxN sera. **(A)** Male WT congenic CD45.1 mice were administered bone-marrow cells from WT or *Ptpra* KO CD45.2 donor mice (WT donors, n=19; KO donors, n=18). **(B)** Male WT (n=11) or *Ptpra* KO (n=11) mice were administered bone-marrow cells from WT congenic CD45.1 mice. Mean ± SEM is shown. *, $p<0.05$, 2way ANOVA. **(C)** WT (n=5) and *Ptpra* KO (n=3) littermate mice were administered Angiosense 680 dye, followed by administration of

K/BxN serum. Ankle fluorescence was monitored after 60 min. Median and IQR is shown. NS, non-significant, Mann-Whitney test. **(D)** WT (n=7) or *Ptpra* KO (n=7) mice were administered K/BxN sera. 8 days post-sera transfer, ankle joints were homogenized and mRNA expression was analyzed by qPCR. Median and IQR is shown. *, $p<0.05$, NS, non-significant, Mann-Whitney test.